Journal of Molecular Spectroscopy **202,** 116–130 (2000)
doi:10.1006/jmsp.2000.8120, available online at http://www.idealibrary.com on IDEAL®

High-Resolution Spectroscopy and *Ab Initio* Calculations on HfCl

R. S. Ram,* A. G. Adam,† A. Tsouli,‡ J. Liévin,‡ and P. F. Bernath*,§

*Department of Chemistry, University of Arizona, Tucson, Arizona 85721; †Department of Chemistry, University of New Brunswick, Fredericton, New Brunswick, Canada E3B 6E2; ‡Université Libre de Bruxelles, Laboratoire de Chimie Physique Moléculaire, CP 160/09, Av. F. D. Roosevelt 50, Bruxelles, Belgium; and §Department of Chemistry, University of Waterloo, Waterloo, Ontario, Canada N2L 3G1

Received February 15, 2000; in revised form March 22, 2000

The emission spectrum of HfCl has been investigated in the 3000–18 500 cm^{-1} region at high resolution using a Fourier transform spectrometer. The bands were excited in a microwave discharge through a flowing mixture of $HfCl_4$ and helium. Two bands near 17 140 and 17 490 cm^{-1} were also measured in absorption using laser excitation spectroscopy. In this instance the molecules were created by laser ablation in a molecular beam apparatus. The observed bands have been classified into two electronic transitions, $[7.6]^4\Delta_{3/2}$–$X^2\Delta_{3/2}$ and $[17.1]^2\Delta_{3/2}$–$X^2\Delta_{3/2}$ involving a common lower state. A rotational analysis of the 0–0 and 1–1 bands of $[7.6]^4\Delta_{3/2}$–$X^2\Delta_{3/2}$ and 0–0, 1–1, and 1–0 bands of the $[17.1]^2\Delta_{3/2}$–$X^2\Delta_{3/2}$ transitions has been carried out and the equilibrium spectroscopic constants have been determined. The ground state principal molecular constants are B_e = 0.1097404(54) cm^{-1}, α_e = 0.0004101(54) cm^{-1}, and r_e = 2.290532(57) Å. *Ab initio* calculations have been performed on HfCl and spectroscopic properties of the low-lying electronic states have been predicted. The ground state is predicted to be a regular $^2\Delta$ state arising from the valence electron configuration, $1\sigma^2 2\sigma^2 3\sigma^2 1\pi^4 1\delta^1$. On the basis of our *ab initio* calculations, we assign the observed transitions as $[7.6]^4\Delta_{3/2}$–$X^2\Delta_{3/2}$ and $[17.1]^2\Delta_{3/2}$–$X^2\Delta_{3/2}$.

INTRODUCTION

Because of the relatively large cosmic abundance of transition metal elements in stars, transition metal-containing molecules are of astrophysical importance. Several transition metal-containing molecules such as oxides (*1–7*) and hydrides (*8–12*) have been identified in the spectra of cool S- and M-type stars and in sunspots. So far no transition metal halides have been identified in stellar spectra, although some metal halides like NaCl, KCl, AlCl, and AlF have been observed in the atmosphere of the carbon star IRC+10216 by millimeter-wave astronomers (*13, 14*). This strengthens the possibility that transition metal chloride and fluoride molecules also might be found. High-quality *ab initio* calculations are now possible for transition metal systems and these predictions should be compared with experiments. For these reasons, there has been a renewed interest in the spectroscopy of transition metal halides (*15–24*). In the IV *B* transition metal family, the electronic spectra of TiF (*25*), TiCl (*26–28*), and ZrCl (*29, 30*) have been studied very recently at high resolution.

The electronic spectrum of HfCl was first observed in 1975 by Kabankova *et al.* (*31*) in absorption. This work was followed by another study by Moskvitina *et al.* (*32*), who confirmed and extended the previous observations and also obtained a rotational analysis of a few bands in the visible region. In this work the technique of intracavity laser spectroscopy was applied and the absorption spectra were recorded in the 560–700 nm region at 0.1 nm/mm dispersion using a grating spectrograph. Although no spin splitting or Ω-doubling was observed, the observed bands were assigned to a $\frac{1}{2}$–$\frac{1}{2}$ transition equivalent to a $^2\Sigma$–$^2\Pi_{1/2}$ transition in Hund's case (a) notation. Among other hafnium-containing halides the spectra of HfBr (*33*) and HfI (*34, 35*) have also been reported, but high-resolution studies are still lacking and the identity of ground state is in question. In the present paper we report on our investigation of HfCl in the 3000–18 500 cm^{-1} region using a Fourier transform spectrometer and by laser excitation spectroscopy. The observed bands have been assigned to two electronic transitions, $[7.6]^4\Delta_{3/2}$–$X^2\Delta_{3/2}$ (6500–7700 cm^{-1}) and $[17.1]^2\Delta_{3/2}$–$X^2\Delta_{3/2}$ (16 000–17 500 cm^{-1}), having a common lower state. The near-infrared transition of HfCl has been observed for the first time. *Ab initio* calculations have also been performed and spectroscopic properties of the low-lying electronic states have been calculated. Our electronic assignments for the observed transitions are supported by these calculations. A rotational analysis of the 0–0 and 1–1 bands of the $[7.6]^4\Delta_{3/2}$–$X^2\Delta_{3/2}$ and 0–0, 1–1, and 1–0 bands of the $[17.1]^2\Delta_{3/2}$–$X^2\Delta_{3/2}$ transitions has been obtained. The results of our experimental and theoretical studies of HfCl are reported in this paper.

EXPERIMENTAL

1. Fourier Transform Spectroscopy

The HfCl molecules were excited in a microwave discharge through a flowing mixture of about 30 mTorr of $HfCl_4$ vapor and 3 Torr of He. The discharge tube was made of quartz and had an outer diameter of 12 mm. The $HfCl_4$ powder was placed in a small bulb, which was heated continuously in order to maintain a constant pressure of $HfCl_4$ vapor in the discharge tube. The HfCl bands appeared strongly when the discharge had an intense blue–white color. The emission from the discharge tube passed directly through the 8-mm entrance aper-

0022-2852/00 $35.00

ture of the 1-m Fourier transform spectrometer of the National Solar Observatory at Kitt Peak. The spectra in the 1800–9000 cm^{-1} interval were recorded using liquid-nitrogen-cooled InSb detectors, Si filters, and a CaF_2 beam splitter. A total of 29 scans were co-added in about 4 h of integration at a resolution of 0.02 cm^{-1}. The 9000–18 500 cm^{-1} range was recorded with Si photodiode detectors, a red pass filter (3–68), and a visible beam splitter. In this case two scans were co-added in 20 min of integration.

The spectral line positions were determined using a data reduction program called PC-DECOMP developed by J. Brault. The peak positions were determined by fitting a Voigt lineshape function to each line. The infrared spectra were calibrated using the wavenumbers of the vibration–rotation lines of the 1–0 band of HCl (*36*), which appeared in emission in the same spectrum. The visible spectra were calibrated with the lines measured by the laser excitation experiment. The molecular lines of HfCl have a typical width of 0.035 cm^{-1} and appear with a maximum signal-to-noise ratio of 8:1 so that the best line positions are expected to be accurate to about ± 0.003 cm^{-1}.

2. *Laser Excitation Spectroscopy*

The apparatus used to create the HfCl molecules in the molecular beam work has been described in detail previously (*21*, *37*); however, some details pertinent to this work will be given. A hafnium target in the form of a slowly rotating and translating rod was ablated by about 3 mJ of 355 nm radiation from a Nd:YAG laser. At the same time, a gas mixture of about 3% $CHCl_3$ seeded in helium was passed from a pulsed molecular beam valve into the ablation region. Vaporized hafnium was entrained by the gas mixture and then expanded through a short expansion channel into a vacuum chamber, producing a molecular beam. HfCl molecules formed through reaction of the hot Hf atoms with the $CHCl_3$ and through condensation during the expansion process. About 5 cm downstream from the nozzle orifice, the molecules were probed with a Coherent 699-29 Autoscan cw ring dye laser. Laser-induced fluorescence was collected orthogonally to both the molecular beam and the probe laser and imaged on a 0.25-m monochromator. Light passing through the monochromator was detected by a cooled photomultiplier. The signal was amplified, integrated, and sent to the computer controlling the Autoscan laser system. R6G laser dye was used to record spectra for the 0–0 and 1–0 bands near 17 140 and 17 490 cm^{-1}, respectively. Typical linewidths were about 180 MHz where the limitation was residual Doppler broadening in the molecular beam. The frequencies of the line positions were measured using the Autoscan system, which has a specified absolute frequency accuracy of ± 200 MHz and a precision of ± 60 MHz.

AB INITIO CALCULATIONS

The electronic structure of HfCl has been investigated by means of large-scale *ab initio* calculations performed on the low-lying states in the doublet and quartet manifolds (eight doublets and four quartets). The *ab initio* approach used in our previous work on transition metal nitrides RuN (*38*), IrN (*39*), and OsN (*40*) has been adopted here. We refer to these papers for more computational details and for an estimate of the accuracy of the calculated spectroscopic properties, typically within 0.05 Å for the equilibrium internuclear distances, within 50 cm^{-1} for harmonic vibrational frequencies, and within 2000 cm^{-1} for the term energy values. The 60 core electrons of Hf have been described by a quasi-relativistic pseudopotential (*41*) and the remaining electrons by the corresponding valence double-zeta (DZ) basis set (*41*), augmented by a single Gaussian *f* function with an exponent of 0.8. By analogy, the Cl atom was represented by a 10-electron quasi-relativistic pseudopotential (*42*) and the corresponding DZ valence basis set (*42*) polarized by a single 3*d* Gaussian primitive with an exponent of 0.75. State-averaged full-valence CASSCF calculations (*43*) were used to optimize the 4σ, 2π, and 1δ valence orbitals correlating with the 5*d* and 6*s* orbitals of hafnium and with the 3*s* and 3*p* orbitals of chlorine. These orbitals were then used in internally contracted multireference configuration interaction calculations (CMRCI) (*44*), in which all valence electrons were correlated. The CMRCI energies were corrected for Davidson's contribution (*45*) for unlinked four-particle clusters. All calculations were performed with the MOLPRO package (*46*) running on the Cray J916 computer and Compaq-Digital Alpha Servers of the ULB/VUB computer center.

The size of the CASSCF wavefunctions ranged between 5000 and 7000 configuration state functions, while CMRCI wavefunctions ranged between 530 000 and 670 000 state functions (for C_{2v} symmetry), depending on the space and spin symmetries.

ELECTRONIC STRUCTURE OF HfCl FROM *AB INITIO* CALCULATIONS

The potential energy curves of 12 electronic states have been calculated in order to get a complete picture of the valence electronic structure of HfCl below 20 000 cm^{-1}. These curves, calculated at the CMRCI level of theory at 12 internuclear distances ranging between 2.0 and 2.75 Å, are shown in Figs. 1–3. The energy scale used in these figures is relative to the minimum energy of the ground electronic state. The relative energies between the different electronic states are better illustrated in Fig. 4, where one observes three clusters of states marked I, II, and III. Cluster I groups the three lowest doublet states below 4000 cm^{-1} states (see Fig. 1); cluster II groups the four lowest quartet states between 7000 and 9000 cm^{-1} (see Fig. 3), and cluster III groups five close-lying doublet states between 16 500 and 18 000 cm^{-1} (see Fig. 2). This clustering can be interpreted by analysis of the CMRCI wavefunctions summarized in Tables 1 and 2, and from the orbital energy diagram of Fig. 5.

Figure 5 has been obtained from full-valence CASSCF calculations performed on the ground states of HfCl ($X^2\Delta$) and of

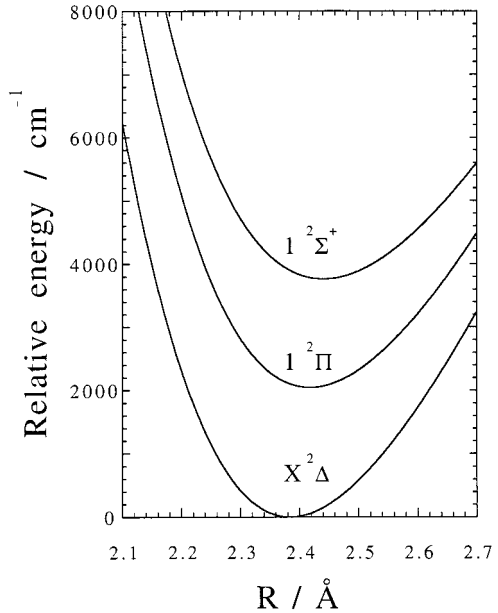

FIG. 1. The doublet potential energy curves of HfCl below 4000 cm^{-1} (cluster I in Fig. 4), from CMRCI calculations.

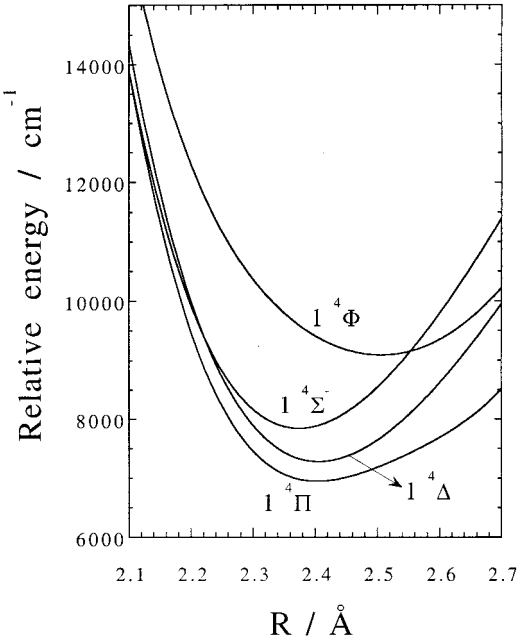

FIG. 3. The quartet potential energy curves of HfCl (cluster II in Fig. 4), from CMRCI calculations.

its dissociation products Hf (^{3}F) and Cl (^{2}P). The energies in this figure are given in electonvolts and are relative to the 1σ orbital of HfCl. One observes a large energy difference between the valence orbitals of Cl and those of Hf, which results in an electronic structure in HfCl that is essentially ionic. An analysis of the CASSCF wavefunction shows indeed that orbitals 1σ, 2σ, and 1π are mainly located on chlorine and the remaining orbitals on hafnium. The dotted lines in the figure give qualitative information on these LCAO mixings. Let us note an important stabilization of the 2σ orbital with respect to the $3p$ orbital of Cl, due to a small bonding contribution from the $5s$ orbital of Hf located 49 eV lower than 1σ. The ionic character can be quantified from the gross Mulliken populations on atoms which predict an $Hf^{+0.55}$ $Cl^{-0.55}$ structure for the

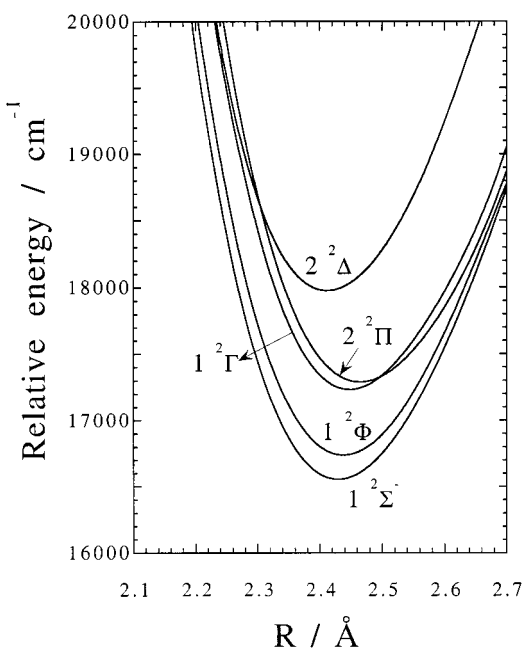

FIG. 2. The doublet potential energy curves of HfCl in the range 16 500–18 000 cm^{-1} (cluster III in Fig. 4), from CMRCI calculations.

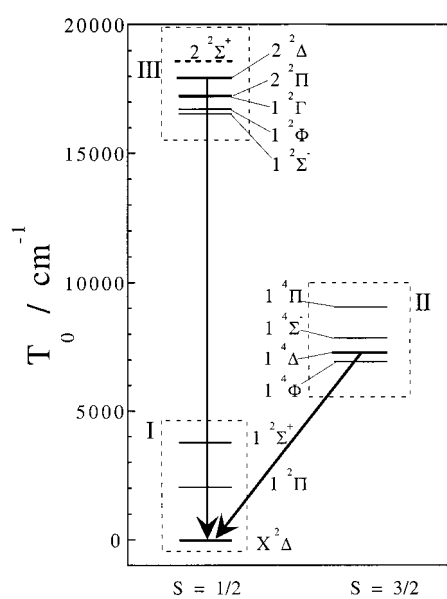

FIG. 4. Relative energies within the doublet and quartet spin systems of HfCl, from CMRCI calculations. The three clusters of levels, labelled to I to III, are detailed in Figs. 1–3. The arrows indicate the two electronic transitions analyzed in this work, as assigned from the *ab initio* calculations.

TABLE 1
Electronic Configurations Describing the Low-Lying Electronic States of HfCl (see Table 2)

Label	Configuration	Electron promotion[a]	Arising states
(A)	$1\sigma^2\,2\sigma^2\,1\pi^4\,3\sigma^2\,1\delta^1$		$^2\Delta$
(B)	$1\sigma^2\,2\sigma^2\,1\pi^4\,3\sigma^2\,2\pi^1$	$1\delta \rightarrow 2\pi$	$^2\Pi$
(C)	$1\sigma^2\,2\sigma^2\,1\pi^4\,3\sigma^2\,4\sigma^1$	$1\delta \rightarrow 4\sigma$	$^2\Sigma+$
(D)	$1\sigma^2\,2\sigma^2\,1\pi^4\,3\sigma^1\,1\delta^1\,2\pi^1$	$3\sigma \rightarrow 2\pi$	$^2\Pi$ (2), $^2\Phi$ (2), $^4\Pi$, $^4\Phi$
(E)	$1\sigma^2\,2\sigma^1\,1\pi^4\,3\sigma^1\,1\delta^2$	$3\sigma \rightarrow 1\delta$	$^2\Gamma$, $^2\Sigma+$, $^2\Sigma-$, $^4\Sigma-$
(F)	$1\sigma^2\,2\sigma^2\,1\pi^4\,3\sigma^1\,1\delta^1\,4\sigma^1$	$3\sigma \rightarrow 4\sigma$	$^2\Delta$ (2), $^4\Delta$
(G)	$1\sigma^2\,2\sigma^2\,1\pi^4\,3\sigma^1\,2\pi^2$	$3\sigma\,1\delta \rightarrow 2\pi^2$	$^2\Delta$, $^2\Sigma+$, $^2\Sigma-$, $^4\Sigma-$
(H)	$1\sigma^2\,2\sigma^2\,1\pi^4\,1\delta^2\,4\sigma^1$	$3\sigma^2 \rightarrow 1\delta\,4\sigma$	$^2\Gamma$, $^2\Sigma+$, $^2\Sigma-$, $^4\Sigma-$
(I)	$1\sigma^2\,2\sigma^2\,1\pi^4\,1\delta^2\,2\pi^1$	$3\sigma^2 \rightarrow 1\delta\,2\pi$	^{2}H, $^2\Phi$, $^2\Pi$ (2), $^4\Pi$
(J)	$1\sigma^2\,2\sigma^2\,1\pi^4\,3\sigma^1\,2\pi^1\,4\sigma^1$	$1\pi\,1\delta \rightarrow 2\pi\,4\sigma$	$^2\Pi$ (2), $^4\Pi$
(K)	$1\sigma^2\,2\sigma^2\,1\pi^4\,3\sigma^1\,4\sigma^2$	$3\sigma\,1\delta \rightarrow 4\sigma^2$	$^2\Sigma+$

[a] Electron promotions are defined with respect to the ground electronic configuration (A).

ground state. More precisely the 11 valence electron charges are distributed over the Hf/Cl atomic orbitals in the following way: 1.62/2.00, 0.31/5.53, and 1.52/0.02, respectively, on *s*, *p*, and *d* orbitals.

The electronic structure of HfCl can be interpreted in terms of 10 configurations listed in Table 1, which are the configurations having a weight greater than 2% in the corresponding CMRCI wavefunctions, as detailed in Table 2. The configuration weights are calculated as the squares of the corresponding CI coefficients. Configurations are labeled from (A) to (J) in Table 1. Configuration (A) $1\sigma^2 2\sigma^2 1\pi^4 3\sigma^2 1\delta^1$ is the ground configuration, leading to a ground $X^2\Delta$ state. Table 1 also gives the electronic states arising from each configuration and the corresponding electron promotion with respect to the ground configuration.

The first set of configurations (A) to (C) are the leading configurations for the states of cluster I. They are characterized by a single electron in the 1δ, 2π, and 4σ orbitals. These orbitals are close in energy (within 2 eV), as can be seen in Fig. 5, and this explains the low term values for the $1^2\Pi$ and $1^2\Sigma^+$ states. Note that the relative energy order for these two states is not correctly predicted by the one electron picture of Fig. 5.

The second set of configurations corresponds to a single pro-

TABLE 2
Analysis of the CMRCI Wavefunctions of HfCl in Terms of Electronic Configurations

Cluster	Electronic state	Weight
I	X $^2\Delta$	84% (A) + 2% (G) + 4% (F)
	1 $^2\Pi$	78% (B) + 9% (D)
	1 $^2\Sigma+$	78% (C) + 8% (H) + 7% (E)
II	1 $^4\Delta$	93% (F)
	1 $^4\Sigma-$	83% (E) + 8% (H)
	1 $^4\Phi$	96% (D)
	1 $^4\Pi$	90% (D) + 5% (J)
III	1 $^2\Sigma-$	68% (E) + 9% (G) + 14% (H)
	2 $^2\Phi$	89% (D)
	1 $^2\Gamma$	90% (E) + 3% (H)
	2 $^2\Pi$	80% (D) + 5% (B)
	2 $^2\Delta$	72% (F) + 11% (G) + 4% (A)
	2 $^2\Sigma+$	34% (E) + 33% (K) + 8% (G)

[a] Weights (in percent) are obtained from the square of the corresponding configuration interaction coefficients; weights lower than 2% are not reported.

[b] See Table 1 for the definition of the configuration labelling.

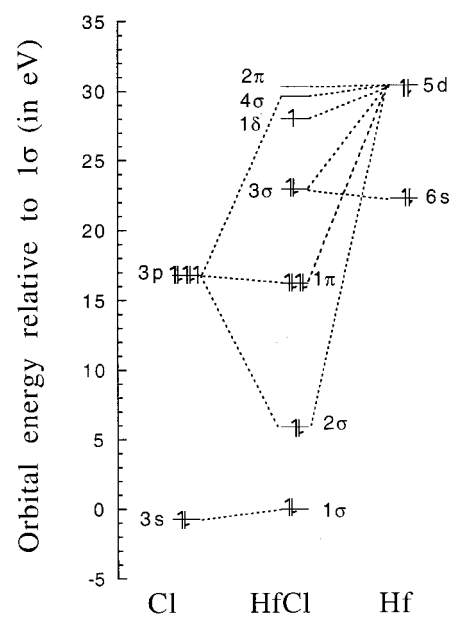

FIG. 5. The molecular orbital correlation diagram for HfCl, from CASSCF calculations performed on the ground states of all species.

motion from the 3σ orbital to the 1δ, 2π, and 4σ orbitals, and therefore larger orbital excitation energies (about 6 eV) than in the case of cluster I. The states arising from these configurations (see Table 1) split into a set of quartets (around 8000 cm^{-1}) and a set of doublet states (around 17 000 cm^{-1}), corresponding, respectively, to clusters II and III. Cluster III contains most of the doublet states arising from configurations (D), (E), and (F), i.e., the $2^2\Pi$ and $1^2\Phi$ (D), $1^2\Gamma$, $1^2\Sigma^-$ and $1^2\Sigma^+$ (E), and $2^2\Delta$ (F) states. The $3^2\Pi$, $2^2\Phi$, and $3^2\Delta$ states lie above 18 000 cm^{-1} and have not been investigated in this work. The $2^2\Sigma^+$ state, indicated with dotted lines in Fig. 4, has been calculated at a single geometry ($R = 2.45$ Å), close to the equilibrium position of most electronic states of HfCl. The relative energy of this state is thus only tentative; the calculated T_e value is 18 490 cm^{-1}.

All the quartet states arising from (D), (E), and (F), i.e., the $1^4\Delta$, $1^4\Sigma^-$, $1^4\Pi$, and $1^4\Phi$, are significantly stabilized (about 10 000 cm^{-1}) with respect to the corresponding doublet states. They form cluster II.

The third set of configurations (G) to (K) are secondary configurations of the states belonging to the three clusters. They have weights ranging between 2 and 14%.

The above analysis thus explains the clustering observed in Fig. 4, in particular the very large gap (about 15 000 cm^{-1}) between both doublet clusters. This analysis also helps in understanding why the ground state of HfCl is a $^2\Delta$ state, and not a $^4\Phi$ state like in the case of the isovalent TiCl molecule (*26–28*).

OBSERVATION AND ANALYSIS

The HfCl bands observed in the 3000–18 500 cm^{-1} region fall into two groups, one in the 6500–7700 cm^{-1} region and the other in the 16 000–17 500 cm^{-1} region, and belong to two transitions with their 0–0 bands near 7634 and 17 040 cm^{-1}, respectively. The 0–0 bands are the most intense in the two systems. A rotational analysis of the two 0–0 bands indicates that they have a common lower state. Following the results of our *ab initio* calculations, we have assigned these two systems as $[7.6]^4\Delta_{3/2}$–$X^2\Delta_{3/2}$ and $[17.1]^2\Delta_{3/2}$–$X^2\Delta_{3/2}$, where the lower state is the ground state of HfCl. For the FT spectra, the rotational lines in 0–0 and 1–1 bands of the two transitions were sorted into branches using a color Loomis–Wood program running on a PC computer. We have determined the molecular constants only for the most abundant $^{180}Hf^{35}Cl$ isotopomer (^{180}Hf and ^{35}Cl have natural abundances of 35 and 76%, respectively). Some weak lines of the $^{180}Hf^{37}Cl$ isotopomer have also been observed, at least in the strong bands, but the data were not sufficient for an independent rotational analysis. The lines involving the less abundant ^{174}Hf (0.2%), ^{176}Hf (5.2%), ^{177}Hf (18.6%), ^{178}Hf (27.3%), and ^{179}Hf (13.6%) isotopes did not usually provide a measurable isotope splitting, so we simply assigned the lines to the main ^{180}Hf isotope.

1. The $[7.6]^4\Delta_{3/2}$–$X^2\Delta_{3/2}$ Transition

The HfCl bands in the 6500–7700 cm^{-1} region have been assigned to the $[7.6]^4\Delta_{3/2}$–$X^2\Delta_{3/2}$ transition. This transition has been observed for the first time. The 0–1, 0–0, and 1–1 bandheads of this transition are located near 7258.9, 7636, and 7609 cm^{-1} with the 0–0 band being the most intense. The 0–1 band is less than 10% of the intensity of the 0–0 band and is overlapped by strong atomic lines. This band was not suitable for rotational analysis. Rotational analysis of only the 0–0 and 1–1 bands was carried out. The rotational structure of these bands consists of only two branches, one *R* and one *P*, consistent with a $\Delta\Omega = 0$ assignment. Our *ab initio* calculation indicates that there are no doublet states in this energy region which could result in a $\Delta\Omega = 0$ transition. Instead, a $^4\Delta$ state has been predicted near 8800 cm^{-1}. This state has four spin components with $\Omega = \frac{1}{2}, \frac{3}{2}, \frac{5}{2}$, and $\frac{7}{2}$. The $^2\Delta$ ground state of HfCl is a regular state with a large spin–orbit splitting of the $\Omega = \frac{5}{2}$ and $\frac{3}{2}$ spin components. In such a case our observed transition can tentatively be assigned as a $\frac{3}{2}$–$\frac{3}{2}$ subband of the $^4\Delta$–$X^2\Delta$ transition. A very weak band has been observed at 6715.7 cm^{-1}, which could be a 0–0 band of the $\frac{5}{2}$–$\frac{5}{2}$ subband. No other bands associated with this transition have been observed in our spectra. An expanded portion of the 0–0 band of the $[7.6]^4\Delta_{3/2}$–$X^2\Delta_{3/2}$ transition is presented in Fig. 6 where the *R* and *P* branches near the *R* head have been marked.

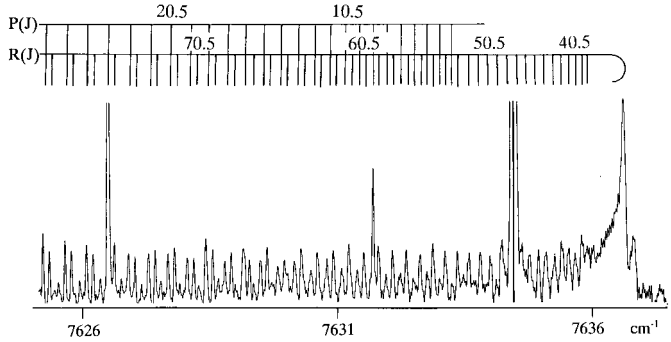

FIG. 6. An expanded portion of the $[7.6]^4\Delta_{3/2}$–$X^2\Delta_{3/2}$ 0–0 band of HfCl near the *R* head.

2. The $[17.1]^2\Delta_{3/2}$–$X^2\Delta_{3/2}$ Transition

The bands belonging to the $[17.1]^2\Delta_{3/2}$–$X^2\Delta_{3/2}$ transition were previously observed by Kabankova *et al.* (*31*) and Moskvitina *et al.* (*32*). Our spectrum consists of $\Delta v = 0$ and $\Delta v = \pm 1$ sequences of this transition with the 0–1, 0–0, and 1–0 *R* heads at 16 764.7, 17 142.1, and 17 493.7 cm^{-1}. The $\Delta v = 0$ sequence is the most intense. The 1–1, 2–2, and 3–3 bandheads of this sequence are located near 17 115.9, 17 089.2, and 17 062.2 cm^{-1}, respectively. All of these bandheads were previously identified by Moskvitina *et al.* (*32*). In the FT spectra, the rotational structure of only the 0–0 and 1–1 bands of this transition was found suitable for a rotational analysis, although the 1–1 band is much weaker than the 0–0 band. The other bands are very weak in intensity and only their bandhead positions could be measured with sufficient precision. A portion of the FT spectrum of the 0–0 sequence is presented in Fig. 7, where *R* heads of the 0–0 and 1–1 bands have been

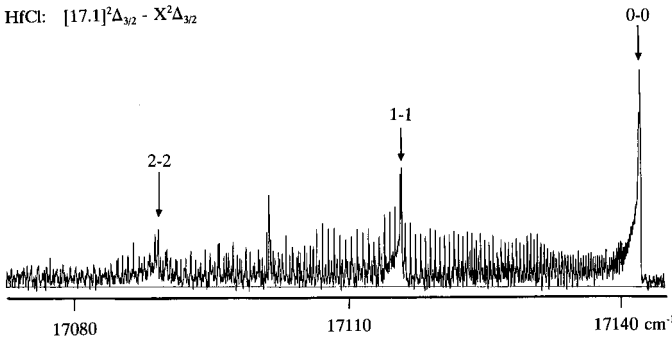

FIG. 7. A compressed portion of the $[17.1]^2\Delta_{3/2}$–$X^2\Delta_{3/2}$ transition of HfCl with the *R* heads of the 0–0, 1–1, and 2–2 bands marked with arrows.

marked. The rotational structure of the 0–0 and 1–1 bands consists of two branches, one *R* and one *P*, again consistent with a $\Delta\Omega = 0$ transition. This transition has been assigned as a $^2\Delta_{3/2}$–$X^2\Delta_{3/2}$ subband of the $[17.1]^2\Delta$–$X^2\Delta$ transition with the help of our *ab initio* calculations. In addition to these bands, there are two very weak heads in the same general region with their *R* heads near 16 896.4 and 16 858.5 cm^{-1}. These bands are possibly the 0–0 and 1–1 bands of the $^2\Delta_{5/2}$–$X^2\Delta_{5/2}$ subband. These new bands were not observed in the absorption spectra of Kabankova *et al.* (*31*) and Moskvitina *et al.* (*32*).

The 0–0 and 1–0 bands of this system of HfCl were also recorded in the molecular beam experiments. The *R*- and *P*-branch lines were readily assigned but the *Q* lines, which were extremely weak in the spectrum, were not assigned until after a fit of the *R* and *P* lines was accomplished. The first *R* and *P* lines were seen confirming the assignment of this transition as $\Omega' = \frac{3}{2}$–$\Omega'' = \frac{3}{2}$. Each band consisted of the resolved lines of at least four isotopomers of HfCl: $^{180}Hf^{35}Cl$, $^{178}Hf^{35}Cl$, $^{180}Hf^{37}Cl$, and $^{178}Hf^{37}Cl$. Only lines for $^{180}Hf^{35}Cl$ and $^{178}Hf^{35}Cl$ were assigned since lines from the less abundant isotopomers were weaker and obscured by their stronger counterparts. A portion of the *R*-head region of the 1–0 band from 17 492 to 17 494 cm^{-1} is shown in Fig. 8. The *R* lines of the $^{180}Hf^{35}Cl$ isotopomer are indicated. For clarity, only the *R* lines near the head for the $^{178}Hf^{35}Cl$ isotopomer are indicated.

The rotational assignments in the different bands of the two transitions were assured by comparing combination differences for the common vibrational levels and the constants were determined by fitting the observed lines to the following simple term energy expression,

$$F_v(J) = T_v + B_v J(J+1) - D_v[J(J+1)]^2. \qquad [1]$$

The rotational assignments were very difficult in the FT spectra because of severe blending in the *R* head and the addition of the laser excitation data overcame this problem. The rotational lines were weighted according to resolution and extent of blending. The observed line positions for the $[7.6]^4\Delta_{3/2}$–$X^2\Delta_{3/2}$ and $[17.1]^2\Delta_{3/2}$–$X^2\Delta_{3/2}$ transitions of $^{180}Hf^{35}Cl$ isotopomer are provided in Table 3, while those of $^{178}Hf^{35}Cl$ isotopomer are provided in Table 4. The molecular constants for the $^{180}Hf^{35}Cl$ and $^{178}Hf^{35}Cl$ isotopomers are provided in Tables 5 and 6, respectively.

DISCUSSION

In our recent studies of TiF (*25*), TiCl (*26*), and ZrCl (*29*), we concluded that the ground states are $^4\Phi$ states. Our assignments were supported by *ab initio* calculations by Harrison on TiF (*47*), and by Boldyrev and Simons (*48*) on TiCl. Focsa *et*

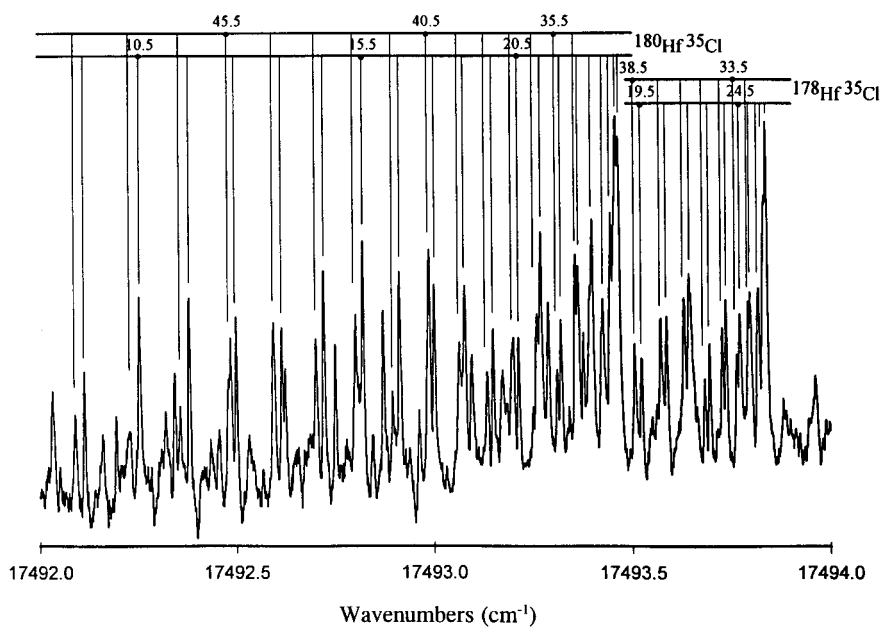

FIG. 8. A portion of the laser excitation spectrum of the 1–0 band near the *R* head. *R* lines of $^{180}Hf^{35}Cl$ and $^{178}Hf^{35}Cl$ isotopomers have been marked.

TABLE 3
Observed Line Positions (in cm^{-1}) of $^{180}Hf^{35}Cl$

J′	J″	Obs.	O-C	J′	J″	Obs.	O-C
			$^{180}Hf^{35}Cl$ $[17.1]^2\Delta$-$X^2\Delta$ 1-1				
15.5	14.5	17114.837	-11	30.5	31.5	17102.354	1
16.5	15.5	17114.959	-1	31.5	32.5	17101.942	7
17.5	16.5	17115.075	9	32.5	33.5	17101.509	-3
19.5	18.5	17115.260	0	33.5	34.5	17101.074	-7
20.5	19.5	17115.352	4	34.5	35.5	17100.638	-7
21.5	20.5	17115.432	3	35.5	36.5	17100.194	-9
22.5	21.5	17115.509	6	36.5	37.5	17099.756	2
23.5	22.5	17115.570	-1	37.5	38.5	17099.306	6
13.5	14.5	17108.490	-2	38.5	39.5	17098.847	8
14.5	15.5	17108.185	4	39.5	40.5	17098.370	-3
15.5	16.5	17107.856	-9	40.5	41.5	17097.895	-5
16.5	17.5	17107.536	-5	41.5	42.5	17097.419	-2
17.5	18.5	17107.201	-10	42.5	43.5	17096.932	-4
18.5	19.5	17106.862	-13	43.5	44.5	17096.451	7
19.5	20.5	17106.536	2	44.5	45.5	17095.951	3
20.5	21.5	17106.172	-13	45.5	46.5	17095.442	-2
21.5	22.5	17105.840	11	46.5	47.5	17094.934	-1
22.5	23.5	17105.478	10	47.5	48.5	17094.416	-4
23.5	24.5	17105.102	1	48.5	49.5	17093.885	-13
24.5	25.5	17104.737	11	49.5	50.5	17093.359	-12
25.5	26.5	17104.345	-1	50.5	51.5	17092.848	10
26.5	27.5	17103.964	4	51.5	52.5	17092.305	6
27.5	28.5	17103.568	0	52.5	53.5	17091.745	-10
28.5	29.5	17103.171	2	53.5	54.5	17091.202	-2
29.5	30.5	17102.768	4	54.5	55.5	17090.649	2
J′	J″	Obs.	O-C	J′	J″	Obs.	O-C
			$^{180}Hf^{35}Cl$ $[17.1]^2\Delta$-$X^2\Delta$ 1-0				
2.5	1.5	17490.770 a	3	44.5	43.5	17492.701 a	-2
3.5	2.5	17490.962 a	1	45.5	44.5	17492.594 a	-1
4.5	3.5	17491.146 a	-2	47.5	46.5	17492.357 a	0
5.5	4.5	17491.329 a	2	48.5	47.5	17492.229 a	1
6.5	5.5	17491.500 a	1	49.5	48.5	17492.090 a	-1
7.5	6.5	17491.667 a	3	50.5	49.5	17491.949 a	2
8.5	7.5	17491.821 a	-1	2.5	3.5	17489.451 a	-2
9.5	8.5	17491.973 a	0	3.5	4.5	17489.210 a	1
10.5	9.5	17492.113 a	-2	4.5	5.5	17488.956 a	-1
11.5	10.5	17492.254 a	2	5.5	6.5	17488.700 a	1
12.5	11.5	17492.380 a	-1	6.5	7.5	17488.430 a	-3
13.5	12.5	17492.500 a	-3	7.5	8.5	17488.160 a	0
14.5	13.5	17492.614 a	-3	8.5	9.5	17487.878 a	-1
15.5	14.5	17492.720 a	-4	9.5	10.5	17487.593 a	2
16.5	15.5	17492.820 a	-4	10.5	11.5	17487.298 a	2
17.5	16.5	17492.913 a	-3	11.5	12.5	17486.993 a	-1
18.5	17.5	17493.001 a	-1	12.5	13.5	17486.689 a	3
19.5	18.5	17493.078 a	-2	13.5	14.5	17486.369 a	0
20.5	19.5	17493.150 a	-2	14.5	15.5	17486.046 a	0
21.5	20.5	17493.213 a	-3	15.5	16.5	17485.715 a	0
22.5	21.5	17493.270 a	-3	16.5	17.5	17485.377 a	0
23.5	22.5	17493.321 a	-1	17.5	18.5	17485.037 a	5
24.5	23.5	17493.364 a	-1	18.5	19.5	17484.682 a	2
25.5	24.5	17493.399 a	0	19.5	20.5	17484.326 a	5
26.5	25.5	17493.426 a	-2	20.5	21.5	17483.955 a	2
27.5	26.5	17493.446 a	-2	21.5	22.5	17483.580 a	0
28.5	27.5	17493.460 a	-2	22.5	23.5	17483.201 a	2

Note. O-C are observed minus calculated wavenumbers in the units of 10^{-3} cm^{-1} and lines marked by "a" were observed in the laser excitation spectra.

al. carried out ligand field calculations on TiCl (*49*) and ZrCl (*50*). We have also observed the doublet–doublet transitions for TiCl (*27*) and ZrCl (*30*). Very recently Sakai *et al.* (*51*) have suggested on the basis of high-quality *ab initio* calculations that the ground state of ZrCl is in fact a $^2\Delta$ state. We have recently carried out our own *ab initio* calculations and some new absorption measurements that are in agreement with this prediction (*52*). A reinterpretation of the doublet states of TiCl

TABLE 3—*Continued*

J′	J″	Obs.	O-C	J′	J″	Obs.	O-C
29.5	28.5	17493.465 a	-3	23.5	24.5	17482.812 a	1
35.5	34.5	17493.357 a	2	24.5	25.5	17482.417 a	1
36.5	35.5	17493.311 a	0	25.5	26.5	17482.013 a	0
37.5	36.5	17493.260 a	-1	26.5	27.5	17481.608 a	4
38.5	37.5	17493.199 a	-3	27.5	28.5	17481.191 a	4
39.5	38.5	17493.135 a	-2	28.5	29.5	17480.767 a	4
40.5	39.5	17493.065 a	0	29.5	30.5	17480.336 a	4
42.5	41.5	17492.896 a	-2	30.5	31.5	17479.896 a	2
43.5	42.5	17492.801 a	-3	31.5	32.5	17479.452 a	3
J′	J″	Obs.	O-C	J′	J″	Obs.	O-C
			$^{180}Hf^{35}Cl$ [17.1]$^2\Delta$-X$^2\Delta$ 0-0				
1.5	1.5	17138.387 a	0	14.5	15.5	17134.304 a	-2
2.5	2.5	17138.369 a	-2	15.5	16.5	17133.993 a	2
3.5	3.5	17138.345 a	-4	16.5	17.5	17133.672 a	3
4.5	4.5	17138.324 a	3	17.5	18.5	17133.338 a	-3
5.5	5.5	17138.292 a	5	18.5	19.5	17133.003 a	-5
6.5	6.5	17138.247 a	0	19.5	20.5	17132.670 a	2
7.5	7.5	17138.200 a	-1	20.5	21.5	17132.326 a	4
8.5	8.5	17138.148 a	1	21.5	22.5	17131.972 a	3
9.5	9.5	17138.088 a	0	22.5	23.5	17131.615 a	4
10.5	10.5	17138.022 a	-2	23.5	24.5	17131.247 a	0
11.5	11.5	17137.951 a	-1	24.5	25.5	17130.878 a	1
12.5	12.5	17137.875 a	1	25.5	26.5	17130.502 a	3
13.5	13.5	17137.792 a	1	26.5	27.5	17130.117 a	1
14.5	14.5	17137.700 a	0	27.5	28.5	17129.726 a	-1
2.5	1.5	17138.920 a	2	28.5	29.5	17129.337 a	5
3.5	2.5	17139.115 a	-1	29.5	30.5	17128.932 a	2
4.5	3.5	17139.311 a	4	30.5	31.5	17128.523 a	1
5.5	4.5	17139.492 a	0	31.5	32.5	17128.111 a	3
6.5	5.5	17139.670 a	0	32.5	33.5	17127.692 a	4
7.5	6.5	17139.844 a	1	33.5	34.5	17127.268 a	6
8.5	7.5	17140.009 a	-1	34.5	35.5	17126.836 a	6
9.5	8.5	17140.168 a	-2	35.5	36.5	17126.396 a	5
10.5	9.5	17140.326 a	3	13.5	14.5	17134.618	3
11.5	10.5	17140.470 a	-1	14.5	15.5	17134.309	3
12.5	11.5	17140.612 a	-1	15.5	16.5	17133.981	-10
13.5	12.5	17140.747 a	-1	16.5	17.5	17133.676	7
14.5	13.5	17140.873 a	-3	17.5	18.5	17133.349	7
15.5	14.5	17140.995 a	-4	18.5	19.5	17133.015	7
16.5	15.5	17141.114 a	-2	19.5	20.5	17132.670	2
17.5	16.5	17141.225 a	-2	20.5	21.5	17132.318	-4
18.5	17.5	17141.332 a	1	21.5	22.5	17131.980	10
19.5	18.5	17141.427 a	-2	22.5	23.5	17131.608	-4
20.5	19.5	17141.518 a	-2	23.5	24.5	17131.245	-2
21.5	20.5	17141.602 a	-4	24.5	25.5	17130.881	4
22.5	21.5	17141.679 a	-6	25.5	26.5	17130.490	-9
23.5	22.5	17141.755 a	-3	26.5	27.5	17130.128	12
24.5	23.5	17141.822 a	-3	27.5	28.5	17129.738	11
25.5	24.5	17141.882 a	-4	28.5	29.5	17129.332	1
26.5	25.5	17141.936 a	-4	29.5	30.5	17128.931	1
27.5	26.5	17141.987 a	-1	30.5	31.5	17128.525	3
28.5	27.5	17142.029 a	-1	31.5	32.5	17128.103	-6
29.5	28.5	17142.058 a	-8	32.5	33.5	17127.697	9
30.5	29.5	17142.092 a	-4	33.5	34.5	17127.267	5
31.5	30.5	17142.113 a	-6	34.5	35.5	17126.824	-6
32.5	31.5	17142.130 a	-6	35.5	36.5	17126.396	4

and ZrCl is also necessary (*52*). A more complete discussion of the experimental and predicted *ab initio* ordering of the electronic states in TiCl, ZrCl, and HfCl will be published separately (*52*).

In contrast to the results obtained for TiCl (*26–28*), our *ab initio* calculations predict a $^2\Delta$ ground state for HfCl with the first quartet state being a $^4\Phi$ state at about 8257 cm^{-1} above the $^2\Delta$ ground state. For ZrCl the $^4\Phi$ and $^2\Delta$ states have almost the same energy with the $^2\Delta$ state a few hundred reciprocal centimeters lower (*51, 52*).

TABLE 3—*Continued*

J′	J″	Obs.	O-C	J′	J″	Obs.	O-C
33.5	32.5	17142.143 a	-4	36.5	37.5	17125.947	1
40.5	39.5	17142.048 a	-1	37.5	38.5	17125.495	-1
41.5	40.5	17142.005 a	-6	38.5	39.5	17125.039	-1
42.5	41.5	17141.962 a	-4	39.5	40.5	17124.584	7
43.5	42.5	17141.917 a	2	40.5	41.5	17124.110	3
44.5	43.5	17141.857 a	-1	41.5	42.5	17123.632	1
45.5	44.5	17141.793 a	-1	42.5	43.5	17123.144	-6
54.5	53.5	17140.944	0	43.5	44.5	17122.657	-6
55.5	54.5	17140.816	-3	44.5	45.5	17122.165	-4
56.5	55.5	17140.680	-7	45.5	46.5	17121.671	1
57.5	56.5	17140.549	0	46.5	47.5	17121.158	-6
58.5	57.5	17140.406	1	47.5	48.5	17120.652	0
59.5	58.5	17140.256	1	48.5	49.5	17120.134	0
60.5	59.5	17140.103	4	49.5	50.5	17119.607	-2
61.5	60.5	17139.933	-3	50.5	51.5	17119.079	0
62.5	61.5	17139.773	5	51.5	52.5	17118.535	-8
63.5	62.5	17139.603	10	52.5	53.5	17118.000	-1
64.5	63.5	17139.423	11	53.5	54.5	17117.452	1
65.5	64.5	17139.237	12	54.5	55.5	17116.902	5
66.5	65.5	17139.039	7	55.5	56.5	17116.331	-5
67.5	66.5	17138.826	-6	56.5	57.5	17115.768	-2
68.5	67.5	17138.632	6	57.5	58.5	17115.193	-4
69.5	68.5	17138.413	-2	58.5	59.5	17114.611	-7
70.5	69.5	17138.205	7	59.5	60.5	17114.030	-2
71.5	70.5	17137.974	1	60.5	61.5	17113.439	-2
72.5	71.5	17137.744	1	61.5	62.5	17112.843	-2
73.5	72.5	17137.514	7	62.5	63.5	17112.241	0
74.5	73.5	17137.275	10	63.5	64.5	17111.628	-4
75.5	74.5	17137.030	14	64.5	65.5	17111.017	0
76.5	75.5	17136.773	12	65.5	66.5	17110.395	0
77.5	76.5	17136.514	13	66.5	67.5	17109.766	-2
78.5	77.5	17136.238	4	67.5	68.5	17109.127	-7
79.5	78.5	17135.961	1	68.5	69.5	17108.490	-5
80.5	79.5	17135.682	1	69.5	70.5	17107.856	6
81.5	80.5	17135.407	11	70.5	71.5	17107.201	3
1.5	2.5	17137.837 a	-2	71.5	72.5	17106.536	-5
2.5	3.5	17137.603 a	-1	72.5	73.5	17105.873	-4
3.5	4.5	17137.365 a	1	73.5	74.5	17105.202	-6
4.5	5.5	17137.116 a	0	74.5	75.5	17104.529	-3
5.5	6.5	17136.864 a	1	75.5	76.5	17103.841	-10
6.5	7.5	17136.605 a	1	76.5	77.5	17103.171	8
7.5	8.5	17136.339 a	1	77.5	78.5	17102.470	1
8.5	9.5	17136.068 a	2	78.5	79.5	17101.767	-4
9.5	10.5	17135.790 a	1	79.5	80.5	17101.055	-10
10.5	11.5	17135.505 a	1	80.5	81.5	17100.350	-3
11.5	12.5	17135.216 a	2	81.5	82.5	17099.628	-8
12.5	13.5	17134.917 a	-1	82.5	83.5	17098.902	-10
13.5	14.5	17134.617 a	2				
J′	**J″**	**Obs.**	**O-C**	**J′**	**J″**	**Obs.**	**O-C**
			$^{180}Hf^{35}Cl$ [7.6]$^4\Delta$-X$^2\Delta$ 1-1				
29.5	28.5	7608.949	6	68.5	67.5	7601.588	1
30.5	29.5	7608.905	-7	69.5	68.5	7601.230	-3
31.5	30.5	7608.866	-6	70.5	69.5	7600.872	3
32.5	31.5	7608.822	-2	9.5	10.5	7603.484	-3
33.5	32.5	7608.771	4	10.5	11.5	7603.186	2
34.5	33.5	7608.701	-2	11.5	12.5	7602.863	-8

The regular $^2\Delta$ ground state of HfCl has a large spin–orbit splitting so that bands involving the excited $X^2\Delta_{5/2}$ spin component would tend to be weak in our spectra. The $X^2\Delta_{5/2}$–$X^2\Delta_{3/2}$ interval could not be determined from our spectra. A group of bands with a very small B value (<0.05 cm^{-1}) have been observed in the 4400–4450 cm^{-1} region. The experimental and chemical evidence suggests that these bands almost certainly involve the Hf atom. These bands are probably due to $HfCl_2$.

As discussed in our papers on TiF (*47*) and TiCl (*26*, *27*), their low-lying electronic states correlate to the states of Ti^+ as do the electronic states of TiH (*53*). A similar correspondence

TABLE 3—*Continued*

J′	J″	Obs.	O-C	J′	J″	Obs.	O-C
35.5	34.5	7608.635	4	12.5	13.5	7602.553	2
36.5	35.5	7608.545	-4	13.5	14.5	7602.232	9
37.5	36.5	7608.464	4	14.5	15.5	7601.895	9
38.5	37.5	7608.367	5	15.5	16.5	7601.538	-3
39.5	38.5	7608.259	2	16.5	17.5	7601.188	0
40.5	39.5	7608.145	3	17.5	18.5	7600.825	-2
41.5	40.5	7608.022	2	18.5	19.5	7600.463	5
42.5	41.5	7607.901	11	19.5	20.5	7600.075	-6
43.5	42.5	7607.758	6	20.5	21.5	7599.693	-2
44.5	43.5	7607.613	9	21.5	22.5	7599.301	-1
45.5	44.5	7607.455	7	22.5	23.5	7598.901	1
46.5	45.5	7607.292	6	23.5	24.5	7598.502	13
47.5	46.5	7607.114	0	24.5	25.5	7598.063	-8
48.5	47.5	7606.935	2	25.5	26.5	7597.652	7
49.5	48.5	7606.745	0	26.5	27.5	7597.219	8
50.5	49.5	7606.542	-6	27.5	28.5	7596.766	-2
51.5	50.5	7606.341	-2	28.5	29.5	7596.320	3
52.5	51.5	7606.134	4	29.5	30.5	7595.856	-2
53.5	52.5	7605.904	-5	30.5	31.5	7595.386	-5
54.5	53.5	7605.686	7	31.5	32.5	7594.904	-12
55.5	54.5	7605.440	-1	32.5	33.5	7594.435	3
56.5	55.5	7605.188	-6	33.5	34.5	7593.934	-7
57.5	56.5	7604.940	0	34.5	35.5	7593.442	1
58.5	57.5	7604.672	-4	35.5	36.5	7592.931	-2
59.5	58.5	7604.406	1	36.5	37.5	7592.420	3
60.5	59.5	7604.123	-2	37.5	38.5	7591.894	1
63.5	62.5	7603.231	-5	38.5	39.5	7591.352	-9
64.5	63.5	7602.923	0	39.5	40.5	7590.822	1
65.5	64.5	7602.602	0	40.5	41.5	7590.267	-4
66.5	65.5	7602.274	2	41.5	42.5	7589.712	-3
67.5	66.5	7601.935	2	43.5	44.5	7588.571	-6
J′	J″	Obs.	O-C	J′	J″	Obs.	O-C
			$^{180}Hf^{35}Cl$ [7.6]$^4\Delta$-$X^2\Delta$ 0-0				
28.5	27.5	7636.602	6	17.5	18.5	7628.418	0
29.5	28.5	7636.576	3	18.5	19.5	7628.059	10
30.5	29.5	7636.545	3	19.5	20.5	7627.667	-3
31.5	30.5	7636.502	-2	20.5	21.5	7627.285	1
32.5	31.5	7636.461	5	21.5	22.5	7626.895	6
33.5	32.5	7636.413	12	23.5	24.5	7626.074	-1
34.5	33.5	7636.342	5	24.5	25.5	7625.659	3
35.5	34.5	7636.261	-4	25.5	26.5	7625.228	-1
36.5	35.5	7636.180	-6	26.5	27.5	7624.792	-1
37.5	36.5	7636.099	3	27.5	28.5	7624.351	1
38.5	37.5	7635.992	-9	28.5	29.5	7623.900	2
39.5	38.5	7635.900	4	29.5	30.5	7623.442	4
40.5	39.5	7635.781	-1	30.5	31.5	7622.975	6
41.5	40.5	7635.662	1	31.5	32.5	7622.498	5
42.5	41.5	7635.535	4	32.5	33.5	7622.012	3
43.5	42.5	7635.386	-7	33.5	34.5	7621.518	1
44.5	43.5	7635.252	5	34.5	35.5	7621.018	3
45.5	44.5	7635.091	-2	35.5	36.5	7620.506	-1
46.5	45.5	7634.935	5	36.5	37.5	7619.987	-3
47.5	46.5	7634.759	0	37.5	38.5	7619.461	-3
48.5	47.5	7634.580	0	38.5	39.5	7618.929	-2
50.5	49.5	7634.189	-9	39.5	40.5	7618.382	-7
51.5	50.5	7633.983	-10	40.5	41.5	7617.820	-19

is expected for HfCl, HfH, and Hf^+ states. The ground state term of Hf^+ is a^2D from the $6s^25d^1$ configuration with a low-lying a^4F ($\sim$6000 cm^{-1}) state from the $6s^15d^2$ configuration (*54*). The ^2D term is split into $X^2\Delta$, $1^2\Pi$, and $1^2\Sigma^+$ states (group I) by the Cl^- ligand field. The ordering of these states is consistent with the effects of the Cl^- anion on the $5d$ electron. Occupation of the $5d\delta$ orbital keeps the d electron away from the ligand and lowers the energy. The a^4F state gives rise to the $^4\Phi$, $^4\Delta$, $^4\Pi$, and $^4\Sigma^-$ states of group II. The a^2D and a^4F states are the low-lying terms for Hf^+ (*54*). The group III states seem to correlate with the ^2G term from the same $6s^15d^2$ configuration of Hf^+ which lies at $\sim$17 500 cm^{-1}.

TABLE 3—*Continued*

J′	J″	Obs.	O-C	J′	J″	Obs.	O-C
52.5	51.5	7633.785	4	41.5	42.5	7617.272	-9
53.5	52.5	7633.562	2	42.5	43.5	7616.707	-9
54.5	53.5	7633.342	11	43.5	44.5	7616.138	-3
55.5	54.5	7633.101	6	44.5	45.5	7615.555	-4
56.5	55.5	7632.857	8	45.5	46.5	7614.965	-3
57.5	56.5	7632.605	9	46.5	47.5	7614.367	-2
58.5	57.5	7632.340	6	47.5	48.5	7613.754	-8
59.5	58.5	7632.062	-2	48.5	49.5	7613.139	-8
60.5	59.5	7631.782	-4	49.5	50.5	7612.521	-2
61.5	60.5	7631.504	6	50.5	51.5	7611.888	-4
62.5	61.5	7631.207	3	51.5	52.5	7611.249	-3
63.5	62.5	7630.903	2	52.5	53.5	7610.598	-7
64.5	63.5	7630.583	-5	53.5	54.5	7609.940	-9
65.5	64.5	7630.265	-4	54.5	55.5	7609.275	-10
66.5	65.5	7629.944	3	55.5	56.5	7608.604	-9
67.5	66.5	7629.609	6	56.5	57.5	7607.932	1
68.5	67.5	7629.264	5	57.5	58.5	7607.233	-10
69.5	68.5	7628.905	0	58.5	59.5	7606.542	-4
70.5	69.5	7628.544	0	59.5	60.5	7605.836	-5
71.5	70.5	7628.183	8	60.5	61.5	7605.134	6
72.5	71.5	7627.798	2	61.5	62.5	7604.406	-1
73.5	72.5	7627.418	9	62.5	63.5	7603.673	-4
74.5	73.5	7627.020	5	63.5	64.5	7602.927	-12
75.5	74.5	7626.617	5	65.5	66.5	7601.434	-5
76.5	75.5	7626.203	3	66.5	67.5	7600.674	-2
77.5	76.5	7625.781	1	67.5	68.5	7599.905	-1
78.5	77.5	7625.353	2	68.5	69.5	7599.128	1
79.5	78.5	7624.916	1	69.5	70.5	7598.342	1
80.5	79.5	7624.468	-2	70.5	71.5	7597.543	-2
81.5	80.5	7624.024	7	71.5	72.5	7596.742	1
82.5	81.5	7623.544	-11	72.5	73.5	7595.931	1
83.5	82.5	7623.088	4	73.5	74.5	7595.110	0
84.5	83.5	7622.607	1	74.5	75.5	7594.282	0
85.5	84.5	7622.117	-3	75.5	76.5	7593.443	-3
86.5	85.5	7621.623	-1	76.5	77.5	7592.603	2
87.5	86.5	7621.118	-2	77.5	78.5	7591.747	-2
88.5	87.5	7620.605	-3	78.5	79.5	7590.886	-2
89.5	88.5	7620.084	-4	79.5	80.5	7590.018	-1
90.5	89.5	7619.553	-7	80.5	81.5	7589.144	2
91.5	90.5	7619.017	-5	81.5	82.5	7588.259	2
94.5	93.5	7617.352	-8	82.5	83.5	7587.360	-3
95.5	94.5	7616.785	-4	83.5	84.5	7586.467	6
96.5	95.5	7616.216	6	84.5	85.5	7585.547	-4
97.5	96.5	7615.618	-3	85.5	86.5	7584.630	-3
98.5	97.5	7615.020	-5	86.5	87.5	7583.702	-4
5.5	6.5	7632.223	-1	87.5	88.5	7582.777	6
6.5	7.5	7631.942	-10	88.5	89.5	7581.826	-2
8.5	9.5	7631.381	-1	89.5	90.5	7580.881	4
9.5	10.5	7631.086	0	90.5	91.5	7579.912	-5
10.5	11.5	7630.785	4	91.5	92.5	7578.952	3
11.5	12.5	7630.462	-6	92.5	93.5	7577.984	10
12.5	13.5	7630.140	-7	93.5	94.5	7576.983	-7
13.5	14.5	7629.820	2	94.5	95.5	7576.004	7
14.5	15.5	7629.482	2	95.5	96.5	7575.004	8
15.5	16.5	7629.144	9	96.5	97.5	7573.995	8
16.5	17.5	7628.783	2				

It is interesting to compare the present results for HfCl with those available for the isoelectronic HfH (*55*). Both of these molecules have a regular $^2\Delta$ ground state. In the HfH case, two $\frac{3}{2}$–$\frac{3}{2}$ transitions (at 14 495 and 19 147 cm^{-1}) showed substantial Ω-doubling in the excited states more consistent with spin components of $^2\Pi$ states. The excited states of both HfH and HfCl evidently have case (c) tendencies and are not well represented by Hund's case (a) labels.

The constants of Table 5 have been used to determine the equilibrium rotational constants for the observed states of $^{180}Hf^{35}Cl$ (Table 7). The equilibrium constants of B_e = 0.1097404(54) cm^{-1}, α_e = 0.0004101(54) cm^{-1} have been obtained for the $X^2\Delta_{3/2}$ ground state, while the values of B_e = 0.105651(54) cm^{-1}, α_e = 0.0004068(67) cm^{-1}, and B_e = 0.1066838(53) cm^{-1}, α_e = 0.0005043(63) cm^{-1} have been determined for $[7.6]^4\Delta_{3/2}$ and $[17.1]^2\Delta_{3/2}$ excited states, respectively.

TABLE 4
Observed Line Positions (in cm^{-1}) of $^{178}Hf^{35}Cl$

J′	J″	Obs.	O-C	J′	J″	Obs.	O-C
			$^{178}Hf^{35}Cl$ $[17.1]^2\Delta$-$X^2\Delta$ 1-0				
2.5	1.5	17491.137 a	0	45.5	44.5	17492.963 a	1
3.5	2.5	17491.329 a	-2	46.5	45.5	17492.845 a	-1
4.5	3.5	17491.520 a	1	1.5	2.5	17490.062 a	4
5.5	4.5	17491.698 a	0	2.5	3.5	17489.821 a	0
6.5	5.5	17491.872 a	1	3.5	4.5	17489.574 a	-3
7.5	6.5	17492.033 a	-3	4.5	5.5	17489.333 a	8
8.5	7.5	17492.195 a	1	5.5	6.5	17489.063 a	-3
9.5	8.5	17492.343 a	-1	6.5	7.5	17488.799 a	0
10.5	9.5	17492.485 a	-2	7.5	8.5	17488.524 a	-2
11.5	10.5	17492.623 a	-1	8.5	9.5	17488.246 a	1
12.5	11.5	17492.750 a	-3	9.5	10.5	17487.954 a	-3
13.5	12.5	17492.872 a	-2	10.5	11.5	17487.664 a	3
14.5	13.5	17492.988 a	-1	11.5	12.5	17487.360 a	1
15.5	14.5	17493.096 a	0	12.5	13.5	17487.049 a	0
16.5	15.5	17493.199 a	3	13.5	14.5	17486.735 a	2
17.5	16.5	17493.289 a	0	14.5	15.5	17486.408 a	0
18.5	17.5	17493.377 a	3	15.5	16.5	17486.078 a	1
19.5	18.5	17493.460 a	7	16.5	17.5	17485.738 a	0
20.5	19.5	17493.523 a	-1	17.5	18.5	17485.398 a	5
21.5	20.5	17493.585 a	-2	18.5	19.5	17485.037 a	-3
22.5	21.5	17493.643 a	-2	19.5	20.5	17484.682 a	2
23.5	22.5	17493.694 a	0	20.5	21.5	17484.318 a	5
24.5	23.5	17493.736 a	0	21.5	22.5	17483.938 a	0
25.5	24.5	17493.771 a	0	22.5	23.5	17483.556 a	-1
26.5	25.5	17493.797 a	-2	23.5	24.5	17483.168 a	0
27.5	26.5	17493.818 a	-2	24.5	25.5	17482.771 a	-1
28.5	27.5	17493.832 a	0	25.5	26.5	17482.366 a	-3
29.5	28.5	17493.838 a	-1	26.5	27.5	17481.965 a	6
33.5	32.5	17493.793 a	1	27.5	28.5	17481.541 a	0
34.5	33.5	17493.764 a	1	28.5	29.5	17481.117 a	1
35.5	34.5	17493.726 a	1	29.5	30.5	17480.686 a	1
36.5	35.5	17493.681 a	0	30.5	31.5	17480.245 a	-1
37.5	36.5	17493.629 a	0	31.5	32.5	17479.799 a	-1
38.5	37.5	17493.571 a	0	32.5	33.5	17479.345 a	-2
43.5	42.5	17493.173 a	1				
J′	J″	Obs.	O-C	J′	J″	Obs.	O-C
			$^{178}Hf^{35}Cl$ $[17.1]^2\Delta$-$X^2\Delta$ 0-0				
2.5	1.5	17138.968 a	3	8.5	8.5	17138.200 a	7
3.5	2.5	17139.163 a	0	9.5	9.5	17138.133 a	0
4.5	3.5	17139.355 a	1	10.5	10.5	17138.066 a	-2
5.5	4.5	17139.538 a	-1	11.5	11.5	17137.995 a	-1
6.5	5.5	17139.718 a	1	12.5	12.5	17137.918 a	0
7.5	6.5	17139.891 a	1	13.5	13.5	17137.834 a	0
8.5	7.5	17140.053 a	-4	14.5	14.5	17137.743 a	0
9.5	8.5	17140.217 a	0	1.5	2.5	17137.884 a	0
10.5	9.5	17140.369 a	-2	2.5	3.5	17137.649 a	0
11.5	10.5	17140.518 a	-1	3.5	4.5	17137.409 a	1
12.5	11.5	17140.661 a	1	4.5	5.5	17137.162 a	1
13.5	12.5	17140.796 a	1	5.5	6.5	17136.906 a	-1
14.5	13.5	17140.922 a	-2	6.5	7.5	17136.647 a	0
15.5	14.5	17141.045 a	-2	7.5	8.5	17136.383 a	2
16.5	15.5	17141.163 a	0	8.5	9.5	17136.109 a	1
17.5	16.5	17141.274 a	0	9.5	10.5	17135.830 a	0
18.5	17.5	17141.379 a	1	10.5	11.5	17135.544 a	-1

Note. O-C are observed minus calculated wavenumbers in the units of 10^{-3} cm^{-1} and lines marked by "a" were observed in the laser excitation spectra.

The equilibrium constants provide the bond lengths of 2.290532(57), 2.334437(60), and 2.323113(58) Å for the $X^2\Delta_{3/2}$, $[7.6]^4\Delta_{3/2}$, and $[17.1]^2\Delta_{3/2}$ states, respectively. The ground state equilibrium bond length can be compared with the bond lengths of 2.2647 Å for the $X^4\Phi$ ground state of TiCl (*26*), 2.3852 Å for the $^4\Phi$ state of ZrCl (*29*), and 2.33 Å for $HfCl_4$ (*56*).

TABLE 4—*Continued*

J′	J″	Obs.	O-C	J′	J″	Obs.	O-C
19.5	18.5	17141.476 a	1	11.5	12.5	17135.255 a	2
20.5	19.5	17141.566 a	-1	12.5	13.5	17134.955 a	-2
21.5	20.5	17141.651 a	-2	13.5	14.5	17134.656 a	3
22.5	21.5	17141.731 a	0	14.5	15.5	17134.340 a	-4
23.5	22.5	17141.805 a	1	15.5	16.5	17134.025 a	-3
24.5	23.5	17141.872 a	1	16.5	17.5	17133.705 a	-1
25.5	24.5	17141.936 a	4	17.5	18.5	17133.376 a	-2
26.5	25.5	17141.987 a	2	18.5	19.5	17133.040 a	-3
27.5	26.5	17142.029 a	-5	19.5	20.5	17132.702 a	-1
28.5	27.5	17142.076 a	0	20.5	21.5	17132.355 a	-1
29.5	28.5	17142.113 a	1	21.5	22.5	17131.999 a	-4
30.5	29.5	17142.143 a	2	22.5	23.5	17131.646 a	3
31.5	30.5	17142.164 a	-1	23.5	24.5	17131.277 a	-2
44.5	43.5	17141.906 a	1	24.5	25.5	17130.907 a	0
45.5	44.5	17141.839 a	-3	25.5	26.5	17130.529 a	-1
46.5	45.5	17141.777 a	4	26.5	27.5	17130.145 a	-1
47.5	46.5	17141.697 a	-1	27.5	28.5	17129.755 a	-1
48.5	47.5	17141.608 a	-8	28.5	29.5	17129.359 a	-1
1.5	1.5	17138.432 a	0	29.5	30.5	17128.958 a	0
2.5	2.5	17138.414 a	-3	30.5	31.5	17128.548 a	-1
3.5	3.5	17138.394 a	-1	31.5	32.5	17128.135 a	1
4.5	4.5	17138.369 a	3	32.5	33.5	17127.714 a	1
5.5	5.5	17138.335 a	2	33.5	34.5	17127.291 a	4
6.5	6.5	17138.292 a	0	34.5	35.5	17126.857 a	3
7.5	7.5	17138.247 a	2	35.5	36.5	17126.412 a	-3

The observed R head positions of 0–1, 1–2, 2–3, 3–4, 0–0, 1–1, 2–2, 3–3, 1–0, 2–1, 3–2, and 4–3 bands at 16 764.7, 16 740.6, 16 716.1, 16 665.7, 17 142.1, 17 115.9, 17 089.2, 17 062.2, 17 493.7, 17 464.8, 17 435.7, and 17 406.1 cm^{-1}, respectively, have been used in the usual vibrational energy expression to determine the vibrational constants of ω_e = 379.85 cm^{-1}, $\omega_e x_e$ = 1.13 cm^{-1} for the $X^2\Delta_{3/2}$ and ω_e = 353.85 cm^{-1}, $\omega_e x_e$ = 1.23 cm^{-1} for the $[17.1]^2\Delta_{3/2}$ state (with T_e = 17 154.10 cm^{-1}). These vibrational constants are in general agreement with those of Moskvitina *et al.* (*32*). Note that the rotational constants of Moskvitina *et al.* (*32*), however, are clearly in error because they predict unreasonably long bond lengths. The equilibrium vibrational constants for the $[7.6]^4\Delta_{3/2}$ state of HfCl could not be determined due to a lack of vibrational bands. The rotational analysis of the 0–0, 1–1, and 1–0 bands of the $[17.1]^2\Delta_{3/2}$–$X^2\Delta_{3/2}$ and 0–0 and 1–1 bands of the $[7.6]^4\Delta_{3/2}$–$X^2\Delta_{3/2}$ transitions provide the $\Delta G'(\frac{1}{2})$ values of 350.3616(25) and 351.85319(86) cm^{-1} for the $[17.1]^2\Delta_{3/2}$ and $[7.6]^2\Delta_{3/2}$ excited states, respectively. The combined fit provides the ground state vibrational interval of $\Delta G''(\frac{1}{2})$ = 377.9694(21) cm^{-1}.

The spectroscopic properties calculated from the CMRCI potential energy curves are given in Table 8, where they are also compared to the available experimental values. The following properties are reported: the equilibrium internuclear distance R_e, the harmonic frequencies at equilibrium ω_e, and the term energies T_0, corrected for the zero-point energy contribution calculated within the harmonic approximation. The calculated values are in good agreement with the corresponding experimental values derived in this work: within 4% for R_e

TABLE 5
Spectroscopic Constants (in cm^{-1}) for the $X^2\Delta_{3/2}$, $[7.6]^4\Delta_{3/2}$, and $[17.1]^2\Delta_{3/2}$ States of $^{180}Hf^{35}Cl$

constants	$X^2\Delta_{3/2}$		$[7.6]^4\Delta_{3/2}$		$[17.1]^2\Delta_{3/2}$	
	v=0	v=1	v=0	v=1	v=0	v=1
T_v	0.0	377.9694(21)	7633.79378(80)	7984.1554(24)	17138.39814(36)	17490.25133(78)
B_v	0.1095353(42)	0.1091252(53)	0.1054479(42)	0.1050411(52)	0.1064316(42)	0.1059273(47)
$10^8 \times D_v$	3.803(37)	4.58(13)	3.951(37)	4.78(12)	3.596(39)	3.27(10)

***Note*:** Numbers in parentheses are one standard deviation in the last digits quoted.

TABLE 6
Spectroscopic Constants (in cm^{-1}) for the $X^2\Delta_{3/2}$ and $[17.1]^2\Delta_{3/2}$ States of $^{178}Hf^{35}Cl$

constants	$X^2\Delta_{3/2}$	$[17.1]^2\Delta_{3/2}$	
	v=0	v=0	v=1
T_v	0.0	17138.44387(37)	17490.62056(44)
B_v	0.1096923(97)	0.1065747(92)	0.1060757(93)
$10^8 \times D_v$	4.07(58)	3.45(52)	3.85(93)

***Note*:** Numbers in parentheses are one standard deviation in the last digits quoted.

(0.09 Å), within 8% (30 cm^{-1}) for ω_e and within 5% (800 cm^{-1}) for the T_0 values. A similar agreement was observed for the two latter properties in the case of diatomic transition metal nitrides calculated at the same level of theory (*37–39*). The agreement was, however, better (within 0.04 Å) for the equilibrium internuclear distances. We attribute this difference to the singly polarized basis set used for the chlorine atom. It was indeed shown (*56–57*) that adding a second 3*d* polarization orbital on third row atoms resulted in a significant lowering of the R_e values, while this effect was negligible in the case of second row atoms. Our *ab initio* calculations thus support the following assignment for the two observed transitions: $1^4\Delta$–$X^2\Delta$ and $2^2\Delta$–$X^2\Delta$ (see the arrows in Fig. 4).

CONCLUSION

The emission spectrum of HfCl has been observed at high resolution using a Fourier transform spectrometer and laser-induced fluorescence in a molecular beam. The bands observed in the 6500–7700 and 16 000–17 500 cm^{-1} regions have been assigned as $[7.6]^4\Delta_{3/2}$–$X^2\Delta_{3/2}$ and $[17.1]^2\Delta_{3/2}$–$X^2\Delta_{3/2}$ transitions. A rotational analysis of the 0–0 and 1–1 bands of the two transitions and the 1–0 band of the $[17.1]^2\Delta_{3/2}$–$X^2\Delta_{3/2}$ transition has been obtained and the molecular constants have been determined. The lowest $^2\Delta$ state has been assigned as the ground state of HfCl consistent with our *ab initio* calculations. The ground state of HfCl ($X^2\Delta_{3/2}$) has a bond length of 2.290532(57) Å to be compared 2.2647 Å for TiCl ($X^4\Phi$) and 2.3852 Å for ZrCl ($^4\Phi$).

TABLE 7
Equilibrium Constants for the $X^2\Delta_{3/2}$, $[7.6]^4\Delta_{3/2}$, and $[17.1]^2\Delta_{3/2}$ States of $^{180}Hf^{35}Cl$

Constants	$X^2\Delta_{3/2}$	$[7.6]^4\Delta_{3/2}$	$[17.1]^2\Delta_{3/2}$
$\Delta G_{1/2}$	377.9694(21)	350.3616(25)	351.85319(86)
B_e	0.1097404(54)	0.1056513(54)	0.1066838(53)
α_e	0.0004101(54)	0.0004068(67)	0.0005043(63)
r_e (Å)	2.290532(57)	2.334437(60)	2.323113(58)

***Note*:** Numbers in parentheses are one standard deviation in the last digits quoted.

TABLE 8
Spectroscopic Properties of the Low-Lying Electronic States of HfCl from CMRCI Calculations

Spin multiplicity	State	T_0 (cm^{-1})	R_e (Å)	ω_e (cm^{-1})
2	$X\ ^2\Delta$	0	2.384	347
			(2.290532)	(379.8)
	$1\ ^2\Pi$	2038	2.417	327
	$1\ ^2\Sigma^+$	3740	2.441	300
	$1\ ^2\Sigma^-$	16540	2.429	318
	$2\ ^2\Phi$	16723	2.436	317
	$1\ ^2\Gamma$	17207	2.454	319
	$2\ ^2\Pi$	17261	2.466	299
	$2\ ^2\Delta$	17955	2.405	338
		(17138)	(2.323113)	(353.8)
4	$1\ ^4\Delta$	7270	2.406	328
		(7634)	(2.334437)	(350.1)
	$1\ ^4\Sigma^-$	7842	2.374	348
	$1\ ^4\Phi$	6915	2.508	259
	$1\ ^4\Pi$	9047	2.404	283

Note. Experimental values from this work are given in parentheses.

ACKNOWLEDGMENTS

We thank J. Wagner, C. Plymate, and M. Dulick of the National Solar Observatory for assistance in obtaining the spectra. The National Solar Observatory is operated by the Association of Universities for Research in Astronomy, Inc., under contract with the National Science Foundation. The research described here was supported by funding from NASA laboratory astrophysics program. Some support was also provided by the Petroleum Research Fund administered by the American Chemical Society and the Natural Sciences and Engineering Research Council of Canada. J.L. thanks the Fonds National de la Recherche Scientifique de Belgique and A.T. thanks the Fondation Van Buuren for financial support.

REFERENCES

1. P. W. Merrill, A. J. Deutsch, and P. C. Keenan, *Astrophys. J.* **136,** 21–34 (1962).
2. H. Machara and Y. Y. Yamashito, *Publ. Astron. Soc. Jpn.* **28,** 135–140 (1976).
3. R. S. Ram, P. F. Bernath, and L. Wallace, *Astrophys. J. Suppl. Ser.* **107,** 443–449 (1996).
4. A. J. Sauval, *Astron. Astrophys.* **62,** 295–298 (1978).
5. S. Wyckoff and R. E. S. Clegg, *Mon. Not. R. Astron. Soc.* **184,** 127–143 (1978).
6. N. M. White and R. F. Wing, *Astrophys. J.* **222,** 209–219 (1978).
7. D. L. Lambert and R. E. S. Clegg, *Mon. Not. R. Astron. Soc.* **191,** 367–389 (1978).
8. R. Yerle, *Astron. Astrophys.* **73,** 346–353 (1979).
9. B. Lindgren and G. Olofsson, *Astron. Astrophys.* **84,** 300–303 (1980).
10. P. K. Carroll, P. McCormack, and S. O'Connor, *Astrophys. J.* **208,** 903–913 (1976).

11. D. L. Lambert and E. A. Mallia, *Mon. Not. R. Astron. Soc.* **151,** 437–447 (1971).
12. O. Engvold, H. Wöhl, and J. W. Brault, *Astron. Astrophys. J. Suppl.* **42,** 209–213 (1980).
13. J. Cernicharo and M. Guélin, *Astron. Astrophys.* **183,** L10–L12 (1987).
14. L. M. Ziurys, A. J. Apponi, and T. G. Phillips, *Astrophys. J.* **433,** 729–732 (1994).
15. E. A. Shenyavskaya, A. J. Ross, A. Topouzhanian, and G. Wannous, *J. Mol. Spectrosc.* **162,** 327–334 (1993).
16. O. Launila, *J. Mol. Spectrosc.* **169,** 373–395 (1995).
17. B. Simard and O. Launila, *J. Mol. Spectrosc.* **168,** 567–578 (1994).
18. O. Launila, B. Simard, and A. M. James, *J. Mol. Spectrosc.* **159,** 161–174 (1993).
19. B. Pouilly, J. Schamps, D. J. W. Lumley, and R. F. Barrow, *J. Phys. B: At., Mol. Opt. Phys.* **11,** 2281–2287 (1978).
20. B. Pouilly, J. Schamps, D. J. W. Lumley, and R. F. Barrow, *J. Phys. B: At., Mol. Opt. Phys.* **11,** 2289–2299 (1978).
21. A. G. Adam, L. P. Fraser, W. D. Hamilton, and M. C. Steeves, *Chem. Phys. Lett.* **230,** 82–86 (1994).
22. R. S. Ram, P. F. Bernath, and S. P. Davis, *J. Mol. Spectrosc.* **173,** 158–176 (1995).
23. C. Dufour, I. Hikmet, and B. Pinchemel, *J. Mol. Spectrosc.* **165,** 398–405 (1994).
24. T. S. Steimle, C. R. Brazier, and J. M. Brown, *J. Mol. Spectrosc.* **110,** 39–52 (1985).
25. R. S. Ram, J. R. D. Peers, Y. Teng, A. G. Adam, A. Muntianu, P. F. Bernath, and S. P. Davis, *J. Mol. Spectrosc.* **184,** 186–201 (1997).
26. R. S. Ram and P. F. Bernath, *J. Mol. Spectrosc.* **186,** 113–130 (1997).
27. R. S. Ram and P. F. Bernath, *J. Mol. Spectrosc.* **195,** 299–307 (1999).
28. T. Imajo, D. Wang, K. Tanaka, and T. Tanaka, "53rd International Symposium on Molecular Spectroscopy, June 1998," Paper MG10.
29. R. S. Ram and P. F. Bernath, *J. Mol. Spectrosc.* **186,** 335–348 (1997).
30. R. S. Ram and P. F. Bernath, *J. Mol. Spectrosc.* **196,** 235–247 (1999).
31. N. N. Kabankova, E. N. Moskvitina, and Y. Y. Kuzyakov, *Vestn. Mosk. Univ., Ser. 2: Khim.* **16,** 232 (1975).
32. E. N. Moskvitina, P. I. Stepanov, and O. B. Shakhovkin, *Spectrosc. Lett.* **20,** 1639–1647 (1993).
33. T. Savithry, D. V. K. Rao, and P. T. Rao, *Physica* **67,** 400 (1973).
34. T. Savithry, D. V. K. Rao, and P. T. Rao, *Curr. Sci. (India)* **40,** 516–518 (1971).
35. T. Savithry, D. V. K. Rao, and P. T. Rao, *Curr. Sci. (India)* **42,** 533–534 (1973).
36. R. B. Le Blanc, J. B. White, and P. F. Bernath, *J. Mol. Spectrosc.* **164,** 574–579 (1994).
37. A. G. Adam and J. R. D. Peers, *J. Mol. Spectrosc.* **181,** 24–32 (1997).
38. R. S. Ram, J. Liévin, and P. F. Bernath, *J. Chem. Phys.* **109,** 6329–6337 (1998).
39. R. S. Ram, J. Liévin, and P. F. Bernath, *J. Mol. Spectrosc.* **197,** 133–146 (1999).
40. R. S. Ram, J. Liévin, and P. F. Bernath, *J. Chem. Phys.* **111,** 3449–3456 (1999).
41. D. Andrea, U. Häussermann, M. Dolg, H. Stoll, and H. Preuss, *Theor. Chim. Acta* **77,** 123 (1990).
42. A. Bergner, M. Dolge, W. Kuechle, H. Stoll, and H. Preuss, *Mol. Phys.* **80,** 1431 (1993).
43. H.-J. Werner and P. J. Knowles, *J. Chem. Phys.* **89,** 5803 (1988); P. J. Knowles and H.-J. Werner, *Chem. Phys. Lett.* **145,** 514 (1988).
44. H.-J. Werner and P. J. Knowles, *J. Chem. Phys.* **82,** 5053 (1985); P. J. Knowles and H.-J. Werner, *Chem. Phys. Lett.* **115,** 259 (1985).
45. S. R. Langhoff and E. R. Davidson, *Int. J. Quantum Chem.* **8,** 62 (1974).
46. [MOLPRO (version 98.1) is a package of *ab initio* programs written by H.-J. Werner and P. J. Knowles, with contributions from J. Almlöf, R. D. Amos, A. Berning, D. L. Cooper, M. J. O. Deegan, A. J. Dobbyn, F. Eckert, S. T. Elbert, C. Hampel, R. Lindh, A. W. Lloyd, W. Meyer, A. Nicklass, K. Peterson, R. Pitzer, A. J. Stone, P. R. Taylor, M. E. Mura, P. Pulay, M. Schütz, H. Stoll, and T. Thorsteinsson.]
47. J. F. Harrison, private communication.
48. A. I. Boldyrev and J. Simons, *J. Mol. Spectrosc.* **188,** 138–141 (1998).
49. C. Focsa, M. Bencheikh, and L. G. M. Pettersson, *J. Phys. B: At. Mol. Phys.* **31,** 2857–2869 (1998).
50. C. Focsa, private communication.
51. Y. Sakai, K. Mogi, and E. Miyoshi, *J. Chem. Phys.* **111,** 299–307 (1999).
52. A. Adam, A. Tsouli, J. Liévin, R. S. Ram, and P. F. Bernath, in preparation.
53. J. Anglada, P. J. Bruna, and S. D. Peyerimhoff, *Mol. Phys.* **69,** 281–303 (1990).
54. C. E. Moore, "Atomic Energy Levels," Vol. III, Natl. Bur. Standards, Washington, DC, 1971.
55. R. S. Ram and P. F. Bernath, *J. Chem. Phys.* **101,** 74–79 (1994).
56. N. Kaltsoyannis, *Chem. Phys. Lett.* **274,** 405–409 (1997).
57. J.-Y. Metz and J. Liévin, *Theor. Chim. Acta* **67,** 369–390 (1985).
58. Y. Kabbadj and J. Liévin, *Phys. Scr.* **40,** 259–269 (1989).